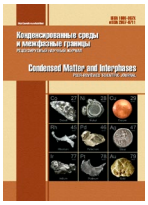

ISSN 1606-867X (Print)
ISSN 2687-0711 (Online)
Condensed Matter and Interphases
Kondensirovannye Sredy i Mezhfaznye Granitsy
https://journals.vsu.ru/kcmf/

Original articles

Research article
https://doi.org/10.17308/kcmf.2025.27/12492

Theoretical and experimental study of the niobium dioxide electronic structure

M. D. Manyakin✉, S. I. Kurganskii, I. S. Kakuliia, S. S. Titova, O. A. Chuvenkova, S. Yu. Turishchev

Voronezh State University,
1 Universitetskaya pl., Voronezh 394018, Russian Federation

Abstract

The investigation of the niobium dioxide electron-energy structure is presented in the paper. The electronic structure computer modeling of the NbO_2 with a rutile crystal structure has been performed using linearized augmented plane wave method. The energy band structure as well as total and partial densities of electronic states are calculated.

Experimental studies of the NbO_2 sample electronic structure were carried out using synchrotron and laboratory X-rays sources. The X-ray photoelectron spectrum of the valence band and subvalent states of NbO_2 and the spectrum of the X-ray absorption near edge structure near K-edge of the oxygen atom in NbO_2 have been recorded.

The spectra of the X-ray absorption near edge structure of the oxygen and niobium atoms K-edges are modeled. The calculated spectra make it possible to reliably interpret the data from the synchrotron experiment. It is shown that for NbO_2 the spectrum calculated for the ground energy state without using the supercell and core hole modeling method demonstrates high agreement with the experiment.

Keywords: Computer modeling, Niobium dioxide, Electronic structure, Density of states, XANES, XPS, Core hole, Rutile

Funding: The study was supported by the Russian Science Foundation grant no. 22-72-00145, https://rscf.ru/project/22-72-00145/.

For citation: Manyakin M. D., Kurganskii S. I., Kakuliia I. S., Titova S. S., Chuvenkova O. A., Turishchev S. Yu. Theoretical and experimental study of the niobium dioxide electronic structure. *Condensed Matter and Interphases*. 2025;27(1): 146–153. https://doi.org/10.17308/kcmf.2025.27/12492

Для цитирования: Манякин М. Д., Курганский С. И., Какулия Ю. С., Титова С. С., Чувенкова О. А., Турищев С. Ю. Теоретическое и экспериментальное исследование электронной структуры диоксида ниобия. *Конденсированные среды и межфазные границы*. 2025;27(1): 146–153. https://doi.org/10.17308/kcmf.2025.27/12492

✉ Maxim D. Manyakin, e-mail: manyakin@phys.vsu.ru

1. Introduction

Materials in which the metal-semiconductor phase transition is observed can be used to create various electronic, optical and other devices: memory elements, neuromorphic hardware devices, "smart windows", devices for energy generation and storage, etc. [1–4]. Such materials include niobium dioxide NbO_2 [3, 5, 6]. Above the phase transition temperature (for NbO_2 Tc ≈ 808 °C), this material has a crystalline structure of the classical rutile type ($P4_2/mnm$ space group) and is a conductor of electric current [7, 8]. Below this temperature, the crystal structure of NbO_2 changes to a distorted rutile structure (space group $I4_1/a$) that accompanied by a change in the nature of the conductivity to semiconducting [7, 8].

In order to study the features of the electron-energy structure of niobium dioxide in the present work a comprehensive study is carried out including the use of ab initio methods of computer modeling, X-ray photoelectron spectroscopy (XPS) and X-ray absorption near edge structure (XANES) spectroscopy.

2. Calculation technique

The high-temperature phase of niobium dioxide has a rutile crystal structure, belongs to tetragonal syngony, and is characterized by the $P4_2/mnm$ space group [3, 7, 9]. The experimental values of the NbO_2 crystal structure parameters given in Table 1 [10] were used in the calculation, similar to other works [9, 11, 12]. The appearance of the NbO_2 unit cell and the corresponding first Brillouin zone are shown in Fig. 1a, b.

Calculations of the electronic structure were performed using the linearized augmented plane waves method using the Wien2k software package [13]. The Generalized Gradient Approximation (GGA) was used to account for the exchange-correlation energy [14]. The radii of muffin-tin spheres R_{mt} given in atomic units of lenght (numerically equal to the Bohr radius a_0), were 1.98 a.u. for the Nb atom and 1.79 a.u. for the O. The $R_{mt} \cdot K_{max}$ value that determines the number of the basis plane waves was 6.0. When integrating over the Brillouin zone 5000 k-points were used for calculating the unit cell and 200 k-points for calculating the supercell.

Table 1. Parameters of the NbO_2 crystal lattice

Space group	$P4_2/mnm$		
Unit cell parameters *a*, *b*, Å	4.8464		
Unit cell parameter *c*, Å	3.0316		
Atomic position	*x/a*	*y/b*	*z/c*
Nb_1	0.0	0.0	0.0
Nb_2	0.5	0.5	0.5
O_1	0.2925	0.2925	0.0
O_2	0.7075	0.7075	0.0
O_3	0.2075	0.7925	0.5
O_4	0.7925	0.2075	0.5

The XANES spectra were modeled for a unit cell in the ground energy state as well as for a 2×2×3 supercell using the core hole method. The formalism of this method is described in detail in our previous work [15]. Previously, this method was successfully tested when calculating the XANES spectra of various oxide materials [16, 17].

3. Experimental technique

The experimental part of the work consisted in conducting studies of the commercial NbO_2 powder sample produced by Sigma-Aldrich [18] using XPS and XANES spectroscopy. X-ray phase analysis of the sample showed that it has a crystalline structure of distorted rutile (space group $I4_1/a$).

The experiments were carried out at the NanoPES synchrotron radiation end-station including the ESCA module of the National Research Center "Kurchatov Institute" [19]. The pressure in the analytical chambers of the NanoPES workstation spectrometers was ~10^{-10} Torr. Electron energy analyzers Specs Phoibos 250 and Phoibos 150 were used. When using a laboratory monochromatic source, the excitation energy was 1486.6 eV.

We used a standard approach to data calibration based on recording the C 1s signal line of hydrocarbon contamination [20]. To compare and analyze the main features of the spectra, well-known databases were used from which the most relevant data were selected [20, 21].

4. Results and discussion

The band structure of NbO_2 is shown in Fig. 1c. The position of the Fermi level (E_F) is selected as the beginning of the energy count. The lower part of the valence band consists of

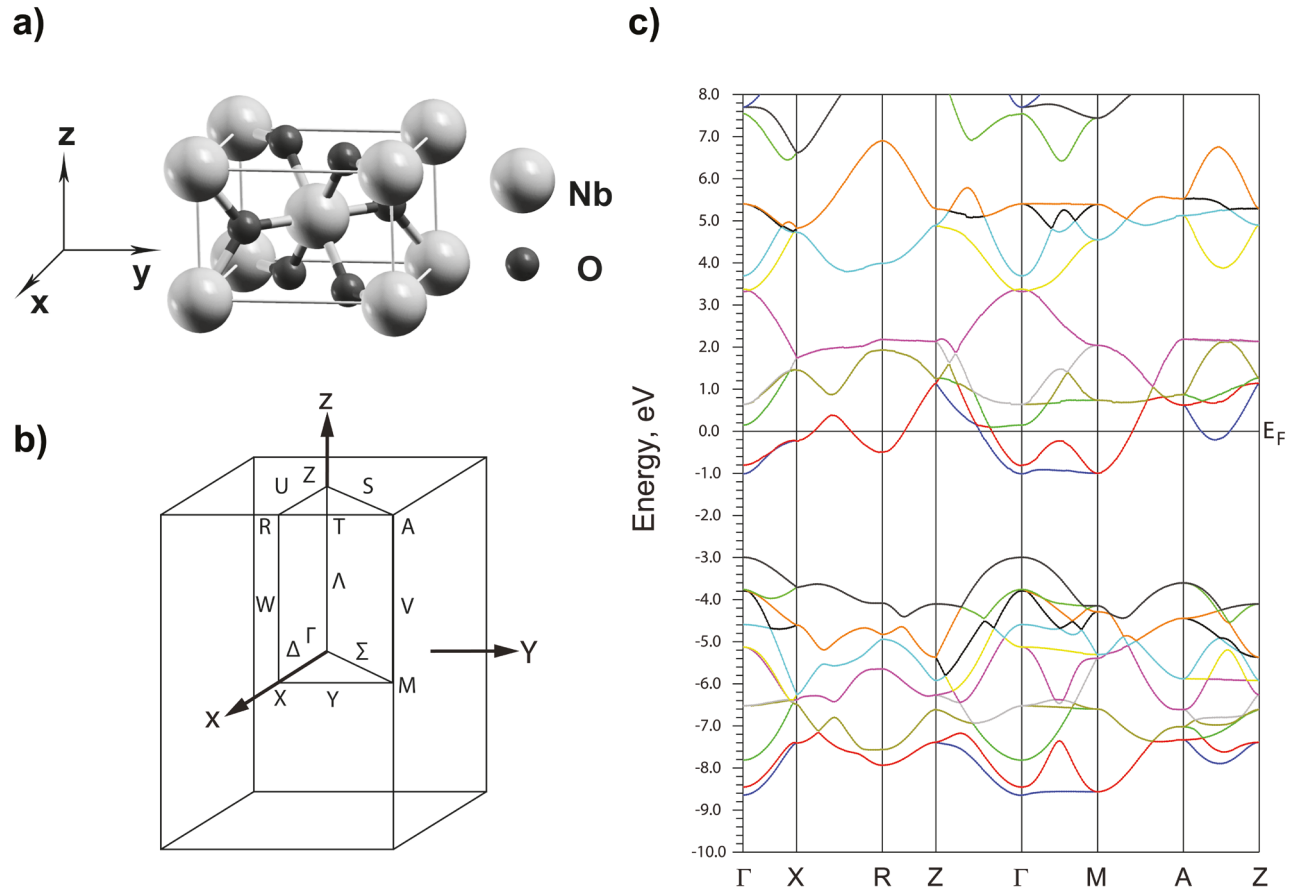

Fig. 1. NbO_2 unit cell with rutile crystalline structure (a). The first Brillouin zone of NbO_2 (b). Band structure of NbO_2 (c)

12 bands originating mainly from 2*p*-states of the oxygen with a small admixture of 4*d*-states of the niobium (see Fig. 2c, d), has a width of 5.65 eV and is located in the energy range of –8.65.. –3.0 eV. Above the top of this group of bands there is a 1.98 eV wide gap of forbidden energies. Even higher in the energy is a group of 10 bands originating mainly from 4*d*-states of niobium atoms with a certain proportion of 2*p*-states of oxygen atoms. According to the crystal field theory due to the octahedral surrounding of the niobium atom by oxygen atoms in NbO_2 the 4*d*-states of Nb are splitted into 6 low-energy bands with t_{2g} symmetry and 4 high-energy bands with e_g symmetry [9]. These two groups of 4*d* bands are well separated in the band structure with the exception of the point Γ vicinity where they slightly overlap [22].

A comparison of the performed calculations results with the data from [8, 9, 11, 22] shows a fairly high agreement which indicates their reliability. At the same time some differences are observed. Compared with the results of [11] there is a noticeable difference in the behavior of the uppermost t_{2g} band in the Z-A and Z-R directions connecting the center of the upper face of the Brillouin zone Z with its vertex A and the middle of its edge R respectively. In both cases the bands have an almost flat character but in our calculation this band lies ~ 1 eV lower in these directions (at an energy of ~ 2.2 eV above E_F) than in [11]. At the same time our picture of the band dispersion of the uppermost t_{2g} band is closest to the results of work [9]. However, in the calculation [9] as in [8] but unlike [11, 22] there is a gap of forbidden energies separating the upper t_{2g} band from the lower e_g band. In our calculation these two groups of bands converge in the vicinity of point Γ similar to the results of [11, 22].

In our calculation the forbidden energy gap dividing the valence band into two parts has a width of 1.98 eV. This is less than the values obtained in other works: 6.1 eV [8], 4.1 eV [22], ~ 3 eV [9].

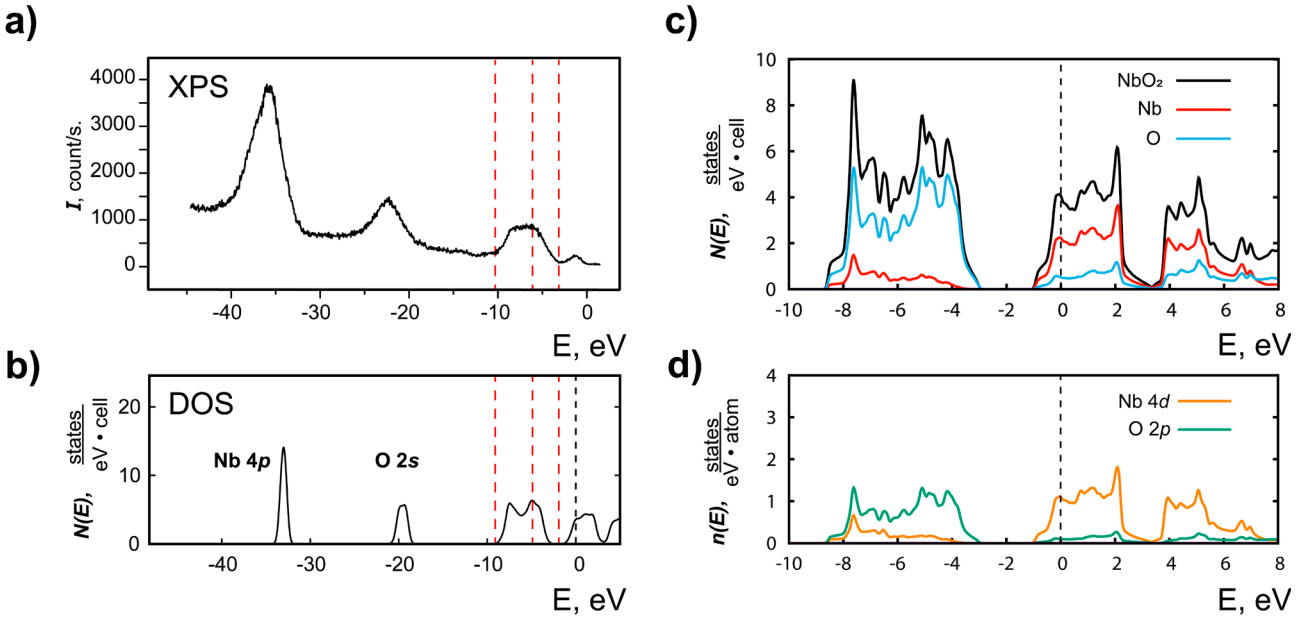

Fig. 2. XPS spectrum of NbO_2 (a). Total DOS of NbO_2 (b). Total DOS of the crystal and the Nb and O atoms in the valence region and near the bottom of the conduction band (c). Partial DOS of the Nb and O atoms (d)

In general, NbO_2 has a band structure typical of rutile-like transition metal oxides. The most important characteristic defining the unusual properties of NbO_2 is the position of the Fermi level which is explained by the following considerations. The free niobium atom has five electrons on the valence shell occupying $4d^4 5s^1$-states. During crystallization into the rutile structure the niobium valence shell electrons are transferring to more electronegative oxygen atoms. Formally the niobium atom in rutile-like NbO_2 has an oxidation state of Nb^{+4} and the filling of the *d*-subshell is $4d^1$ [23]. As a result, the energy bands formed from the *d*-states of niobium atoms are partially occupied by electrons. The Fermi level crosses a group of bands formed by Nb *4d*-states which acts as a conduction band and NbO_2 exhibits a metallic type of electrical conductivity.

The results of NbO_2 XPS spectroscopy provide important information about the features of occupied electronic states. Fig. 2a shows the X-ray photoelectron spectrum of the NbO_2 sample recorded in the range of binding energies from –45 to 0 eV. In the considered energy range 4 regions of occupied states are observed similar to the results of [24] and the experimental spectrum is generally consistent with the results of [11, 24–28]. The XPS spectrum was compared with the total density of states calculation results in the same energy range by combining the position of the valence band on the energy scale (Fig. 2b). At the same time the starting point of the experimental and calculated scales do not coincide. Fig. 2a, b shows a good agreement of the results which makes it possible to explain the features observed in the XPS spectrum. The intense peak at –35.8 eV in the experimental spectrum corresponds to the density of Nb 4*p*- states peak at the –33.0 eV on the calculation scale where the position of the Fermi level is taken as the starting point. The experimental peak at –22.25 eV corresponds to the density of O 2*s*- states peak at an energy of –19.5 eV on the calculation scale. The peaks position of the Nb 4*p*- and O 2*s*- states in the calculation turns out to be shifted closer to the Fermi level if compared with the experiment. At the same time the distance between the peaks in the calculation is 13.5 eV which is in excellent agreement with the experimental value of 13.55 eV.

Features in the energy range –10 .. 0 eV describes the structure of the valence band. This area as well as the bottom of the conduction band are shown on an enlarged scale in Fig. 2c, d. The total density of electronic states (DOS) of the NbO_2 crystal, the total atomic DOS for Nb

and O atoms as well as the partial densities for Nb 4*d*- and O 2*p*- electronic states dominating in the considered energy range are shown. As mentioned above the valence band consists of two regions. Its lower part from –8.65 to –3.0 eV is formed mainly by 2*p*-oxygen states. Nb 4*d*-states dominate in the upper part of the valence band and at the bottom part of the conduction band in the range from –1 to +6 eV. It can be seen that there is a contribution of O 2*p*-states to the two upper groups of bands and Nb 4*d*-states to the lower group respectively that indicates the covalent component of the chemical bond [9]. In the low-energy group of states there are local maxima at the bottom and top of the considered range with the local minimum observed in its center. The Fermi level is located near the local DOS maximum which may indicate the instability of such an electronic structure and contribute to the metal–semiconductor phase transition observed in NbO_2. The calculated DOS spectra are in good agreement with the results of [11, 22].

Figure 3 shows a comparison of the experimentally recorded O K-edge XANES spectrum with the spectra calculated for a unit cell in the ground energy state (without core hole modeling) and for a 2×2×3 supercell calculated using the core hole method. The experimental spectrum contains three maxima designated as A, B and C at energies 531.1, 534.8, and 542.0 eV, respectively. Maximum A has the highest intensity. The intensities of maxima B and C are approximately equal. Experimental spectra of the O K-edge with the same intensity ratio between the maxima were obtained in [27] by the XANES method for NbO_2 thin films and in [12] by electron energy loss spectroscopy (EELS) for a commercial sample produced by Alfa Aesar. The relative intensity of peak A is less than the intensity of peak B but greater than the intensity of peak C in spectra obtained by EELS for commercial samples produced by Aldrich [29] and Alfa Aesar samples [30]. It can be concluded that the data presented in the literature are ambiguous and probably depend on the conditions of the experiment as well as the subsequent mathematical processing of the result.

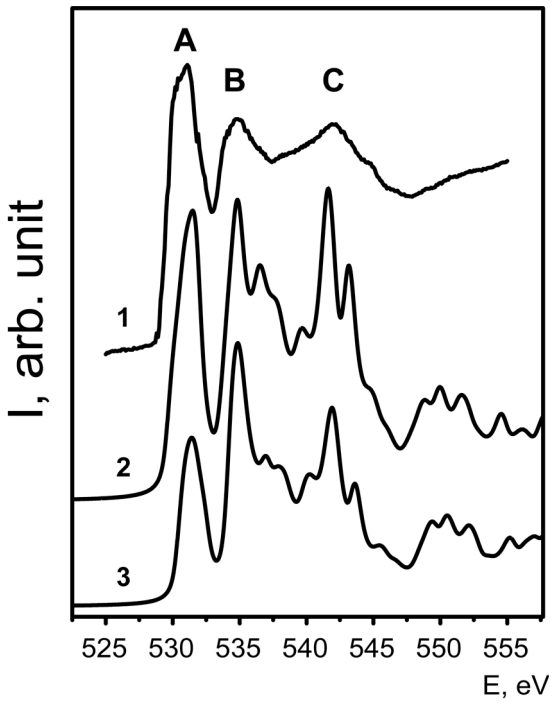

Fig. 3. O K-edge XANES spectrum. *1* – experimental, *2* – calculation for unit cell without core hole, *3* – calculation for supercell with core hole

The calculated spectra shown in Fig. 3 were compared with the experimental one based on the maximum B position at an energy of 534.8 eV. In our calculation performed for a unit cell in the ground energy state all three maxima have a similar intensity, but maximum A has the lowest value and maximum C has the highest. There are known papers [12, 27] in which calculations of the O K absorption edge were also performed using the Wien2k software package. In [27] the ratio of the maxima A and B have the same intensities as ours but unlike our result in [27] maximum C has the lowest intensity. In [12] maximum A is the most intense followed by least intense maximum B and C. Thus, in all three calculations including the present one the obtained results differ slightly in the ratio of the main spectrum features intensities. At the same time there is a good agreement between the calculated spectra and the experimental one in terms of the number of peaks and their position on the energy scale that makes it possible to unambiguously interpret the experimental data.

The use of the core hole method in the calculation does not lead to a change in the number of features in the spectrum or their position on the energy scale. However, the

relative intensity of the A and C maxima is noticeably decreasing. The decrease of the first peak intensity in the calculated XANES O K-edge spectrum by the core hole method in transition metal oxides is a well-known effect [31]. According to our calculations and ones given in [23, 31] the hybridization of unoccupied O2*p*-electronic states and unoccupied states of metal atoms is observed in transition metal oxides. According to this approach the O K spectrum fine structure is explained as follows. Peak A in the spectrum reflects the density of oxygen 2*p*- states hybridized with niobium t_{2g} states, peak B – with niobium e_g states. Peak C reflects the hybridization of O 2*p*- states and 5*s*-, 5*p*- metal states. Thus, modeling a core hole leads to a systematic underestimation of the first peak intensity associated with t_{2g}-symmetry states [31].

Using the XANES O K spectrum as the example we conclude that the calculation for the NbO_2 unit cell without accounting the core hole gives results that are better consistent with experiment. Therefore, for the Nb K absorption edge the calculation was performed only for the unit cell. The result in comparison with the experimental spectrum [32] is given in Fig. 4. The calculated spectrum reproduces all the absorption edge fine structure main features presented in the experimental spectrum which indicates the correctness of the chosen modeling method and the reliability of the result obtained.

5. Conclusions

The electronic structure of niobium dioxide has been studied by the linearized augmented plane waves method. The band structure, total and partial densities of electronic states are calculated. The DOS spectrum allows reliable interpretation of XPS spectroscopy results.

The results of XANES spectra calculations for the Nb K-, O K- absorption edges are presented. For the O K absorption edge spectrum it is shown that the calculation for the ground energy state without using the supercell and core hole modeling method demonstrates high agreement with the synchrotron experiment.

The results obtained can be used in the analysis of experimentally studied samples of the Nb – O system.

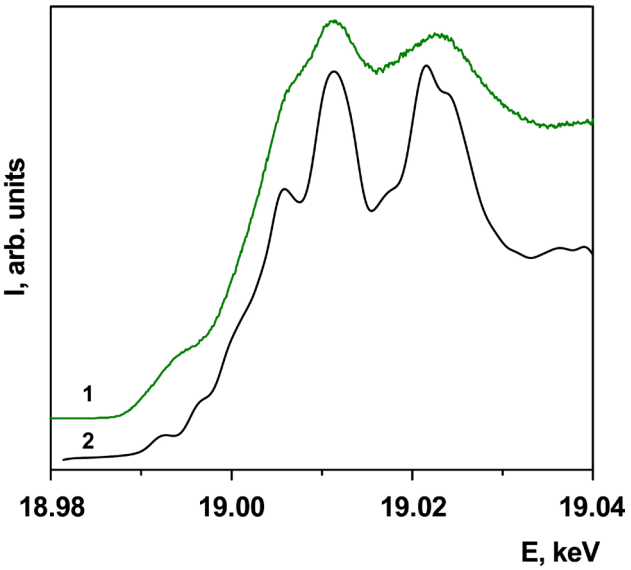

Fig. 4. Nb K-edge XANES spectrum. 1 – experimental [32], 2 – our calculation.

Contribution of the authors

All authors made an equivalent contribution to the preparation of the publication.

Conflict of interests

The authors declare that they have no known competing financial interests or personal relationships that could have appeared to influence the work reported in this paper.

References

1. Zhou Y., Ramanathan S. Mott memory and neuromorphic devices. *Proceedings of the IEEE*. 2015;103(8): 1289–1310. https://doi.org/10.1109/JPROC.2015.2431914

2. Joshi T., Cirino E., Morley S. A., Lederman D. Thermally induced metal-to-insulator transition in NbO_2 thin films: modulation of the transition temperature by epitaxial strain. *Physical Review Materials*. 2019;3: 124602. https://doi.org/10.1103/PhysRevMaterials.3.124602

3. Music D., Krause A. M., Olsson P. A. T. Theoretical and experimental aspects of current and future research on NbO_2 thin film devices. *Crystals*. 2021;11: 217. https://doi.org/10.3390/cryst11020217

4. Manning T. D., Parkin I. P., Pemble M. E., Sheel D., Vernardou D. Intelligent window coatings: atmospheric pressure chemical vapor deposition of tungsten-doped vanadium dioxide. *Chemistry of Materials*. 2004;16(4): 744–749. https://doi.org/10.1021/cm034905y

5. Fajardo G. J. P., Howard S. A., Evlyukhin E., ... Piper L. F. J. Structural phase transitions of NbO_2: bulk versus surface. *Chemistry of Materials*. 2021;33: 1416–1425. https://doi.org/10.1021/acs.chemmater.0c04566

6. Park J., Hadamek T., Posadas A. B., Cha E., Demkov A. A., Hwang H. Multi-layered $NiO_y/NbO_x/NiO_y$ fast drift-free threshold switch with high I_{on}/I_{off} ratio for selector

application. *Scientific Reports*. 2017;7: 4068. https://doi.org/10.1038/s41598-017-04529-4

7. Shapiro S. M., Axe J. D., Shirane G., Raccah P. M. Neutron scattering study of the structural phase transition in NbO_2. *Solid State Communications*. 1974;15: 377–381. https://doi.org/10.1016/0038-1098(74)90780-7

8. Posternak M., Freeman A. J., Ellis D. E. Electronic band structure, optical properties, and generalized susceptibility of NbO_2. *Physical Review B*. 1979;19: 6555–6563. https://doi.org/10.1103/PhysRevB.19.6555

9. Eyert V. The metal-insulator transition of NbO_2: an embedded Peierls instability. *Europhysics Letters*. 2002;58: 851–856. https://doi.org/10.1209/epl/i2002-00452-6

10. Bolzan A. A., Fong C., Kennedy B. J., Howard C. J. Structural studies of rutile-type metal dioxides. *Acta Crystallographica*. 1997;B53: 373–380. https://doi.org/10.1107/S0108768197001468

11. O'Hara A., Nunley T. N., Posadas A. B., Zollner S., Demkov A. A. Electronic and optical properties of NbO_2. *Journal of Applied Physics*. 2014;116: 213705. https://doi.org/10.1063/1.4903067

12. Jiang N., Spence J. C. H. Electron energy-loss spectroscopy of the O K edge of NbO_2, MoO_2, and WO_2. *Physical Review B*. 2004;70: 245117. https://doi.org/10.1103/PhysRevB.70.245117

13. Blaha P., Schwarz K., Tran F., Laskowski R., Madsen G.K.H., Marks L.D. WIEN2k: An APW+lo program for calculating the properties of solids. *The Journal of Chemical Physics*. 2020;152: 074101. https://doi.org/10.1063/1.5143061

14. Perdew J. P., Burke K., Ernzerhof M. Generalized gradient approximation made simple. *Physical Review Letters*. 1996;77: 3865-3868. https://doi.org/10.1103/PhysRevLett.77.3865

15. Manyakin M. D., Kurganskii S. I. Electronic structure of germanium dioxide with rutile structure according to ab initio computer simulation data. *Condensed Matter and Interphases*. 2023;25(4): 587–593. https://doi.org/10.17308/kcmf.2023.25/11478

16. Manyakin M. D., Kurganskii S. I. Electronic structure of stishovite SiO_2. *Journal of Physics: Conference Series*. 2019;1352: 012032. https://doi.org/10.1088/1742-6596/1352/1/012032

17. Turishchev S., Schleusener A., Chuvenkova O., ... Sivakov V. Spectromicroscopy studies of silicon nanowires array covered by tin oxide layers. *Small*. 2023;19(10): 2206322. https://doi.org/10.1002/smll.202206322

18. https://www.sigmaaldrich.com/RU/en

19. Lebedev A. M., Menshikov K. A., Nazin V. G., Stankevich V. G., Tsetlin M. B., Chumakov R. G. NanoPES photoelectron beamline of the Kurchatov synchrotron radiation source. *Journal of Surface Investigation: X-ray, Synchrotron and Neutron Techniques*. 2021;15(5): 1039–1044. https://doi.org/10.1134/S1027451021050335

20. Moulder J. F., Stickle W. F., Sobol P. E., Bomben K. D. *Handbook of X-ray photoelectron spectroscopy. Physical Electronics Division*. Eden Prairie, Minnesota: Perkin-Elmer Corporation; 1992. 261 p.

21. Crist B. V. *Handbook of Mmonochromatic XPS Spectra: the elements of native oxides*. Mountain View: Wiley; 2000. 500 p.

22. Xu J. H., Jarlborg T., Freeman A. J. Self-consistent band structure of the rutile dioxides NbO_2, RuO_2, and IrO_2. *Physical Review B*. 1989;40: 7939–7949. https://doi.org/10.1103/PhysRevB.40.7939

23. Frati F., Hunault M. O. J. Y., de Groot F. M. F. Oxygen K-edge X-ray absorption spectra. *Chemical Reviews*. 2020;120(9): 4056–4110. https://doi.org/10.1021/acs.chemrev.9b00439

24. Kuznetsov M. V., Razinkin A. S., Shalaeva E. V. Photoelectron spectroscopy and diffraction of surface nanoscale NbO/Nb(110) structures. *Journal of Structural Chemistry*. 2009;(50): 514–521. https://doi.org/10.1007/s10947-009-0079-y

25. Beatham N., Orchard A. F. X-ray and UV photoelectron spectra of the oxides NbO_2, MoO_2 and RuO_2. *Journal of Electron Spectroscopy and Related Phenomena*. 1979;16: 77–86. https://doi.org/10.1016/0368-2048(79)85006-9

26. Fujiwara K., Tsukazaki A. Formation of distorted rutile-type NbO_2, MoO_2, and WO_2 films by reactive sputtering. *Journal of Applied Physics*. 2019;125: 085301. https://doi.org/10.1063/1.5079719

27. Wahila M. J., Paez G., Singh C. N., ... Piper L. F. J. Evidence of a second-order Peierls-driven metal-insulator transition in crystalline NbO_2. *Physical Review Materials*. 2019;3: 074602. https://doi.org/10.1103/PhysRevMaterials.3.074602

28. Berman S., Zhussupbekova A., Boschker J. E., ... Zhussupbekov K. Reconciling the theoretical and experimental electronic structure of NbO_2. *Physical Review B*. 2023;108: 155141. https://doi.org/10.1103/PhysRevB.108.155141

29. Arnold A., Tao R., Klie R. F. Comparison of FEFF9 results of metallic niobium and niobium oxides to EELS. *Journal of Undergraduate Research*. 2012;5(1): 38–41. https://doi.org/10.5210/JUR.V5I1.7508

30. Bach D., Schneider R., Gerthsen D., Verbeeck J., Sigle W. EELS of niobium and stoichiometric niobium-oxide phases – part I: plasmon and near-edges fine structure. *Microscopy and Microanalysis*. 2009;15(6): 505–523. https://doi.org/10.1017/S143192760999105X

31. Liang Y., Vinson J., Pemmaraju S., Drisdell W. S., Shirley E. L., Prendergast D. Accurate X-ray spectral predictions: an advanced self-consistent-field approach inspired by many-body perturbation theory. *Physical Review Letters*. 2017;118: 096402. https://doi.org/10.1103/physrevlett.118.096402

32. Sahiner M. A., Nabizadeh A., Rivella D., Cerqueira L., Hachlica J., Morea R., Gonzalo J., Woicik J. C. Subtle local structural variations in oxygen deficient niobium germanate thin film glasses as revealed by x-ray absorption spectroscopy. *Journal of Physics: Conference Series*. 2016;712: 012103. https://doi.org/10.1088/1742-6596/712/1/012103

Information about the authors

Maxim D. Manyakin, Cand. Sci. (Phys.-Math.), Researcher, Joint Scientific and Educational Laboratory "Atomic and Electronic Structure of Functional Materials" of Voronezh State University and the National Research Center «Kurchatov institute», Voronezh State University (Voronezh, Russian Federation).
https://orcid.org/0000-0003-2260-6233
manyakin@phys.vsu.ru

Sergey I. Kurganskii, Dr. Sci. (Phys.-Math.), Professor of the Solid State Physics and Nanostructure Department, Voronezh State University (Voronezh, Russian Federation).
kurganskii@phys.vsu.ru

Iuliia S. Kakuliia, Teacher of General Physics Department, Voronezh State University (Voronezh, Russian Federation).
https://orcid.org/0000-0002-0953-9024
kakuliia@phys.vsu.ru

Sofiia S. Titova, Teacher of General Physics Department, Voronezh State University, (Voronezh, Russian Federation).
https://orcid.org/0000-0001-6860-401X
titova@phys.vsu.ru

Olga A. Chuvenkova, Cand. Sci. (Phys.-Math.), Senior Researcher, Joint Scientific and Educational Laboratory «Atomic and Electronic Structure of Functional Materials» of Voronezh State University and the National Research Center «Kurchatov Institute», Voronezh State University (Voronezh, Russian Federation).
https://orcid.org/0000-0001-5701-6909
chuvenkova@phys.vsu.ru

Sergey Yu. Turishchev, Dr. Sci. (Phys.-Math.), Associate Professor, Head of the General Physics Department, Voronezh State University (Voronezh, Russian Federation).
https://orcid.org/0000-0003-3320-1979
tsu@phys.vsu.ru

Received 02.04.2024; approved after reviewing 23.04.2024; accepted for publication 08.05.2024; published online 25.03.2025.

Translated by Sergey Turishchev